AGU PUBLICATIONS

Geophysical Research Letters

RESEARCH LETTER
10.1002/2016GL072101

Key Points:
- Salinity minima have been observed in the thermocline of the Baltic Sea at high resolution
- The salinity minima are explained by the joint action of offshore Ekman transport and surface warming
- In large-scale upwelling systems salinity inversions may be salinity maxima, due to due to less saline upwelling waters

Correspondence to:
H. Burchard,
hans.burchard@io-warnemuende.de

Citation:
Burchard, H., N. B. Basdurak, U. Gräwe, M. Knoll, V. Mohrholz, and S. Müller (2017), Salinity inversions in the thermocline under upwelling favorable winds, *Geophys. Res. Lett.*, *44*, doi:10.1002/2016GL072101.

Received 29 NOV 2016
Accepted 17 JAN 2017
Accepted article online 19 JAN 2017

Salinity inversions in the thermocline under upwelling favorable winds

Hans Burchard[1], N. Berkay Basdurak[1], Ulf Gräwe[1,2], Michaela Knoll[3], Volker Mohrholz[1], and Selina Müller[1]

[1]Leibniz Institute for Baltic Sea Research Warnemünde, Rostock, Germany, [2]Institute of Meteorology and Climatology, Leibniz-Universität Hannover, Hanover, Germany, [3]Bundeswehr Technical Centre for Ships and Naval Weapons, Maritime Technology and Research (WTD 71), Eckernförde, Germany

Abstract This paper discusses and explains the phenomenon of salinity inversions in the thermocline offshore from an upwelling region during upwelling favorable winds. Using the nontidal central Baltic Sea as an easily accessible natural laboratory, high-resolution transect and station observations in the upper layers are analyzed. The data show local salinity minima in the strongly stratified seasonal thermocline during summer conditions under the influence of upwelling favorable wind. A simple analytical box model using parameters (including variation by means of a Monte Carlo method) estimated from a hindcast model for the Baltic Sea is constructed to explain the observations. As a result, upwelled water with high salinity and low temperature is warmed up due to downward surface heat fluxes while it is transported offshore by the Ekman transport. The warming of upwelled surface water allows maintenance of stable stratification despite the destabilizing salinity stratification, such that local salinity minima in the thermocline can be generated. Inspection of published observations from the Benguela, Peruvian, and eastern tropical North Atlantic upwelling systems shows that also there salinity inversions occur in the thermocline, but in these cases thermocline salinity shows local maxima, since upwelled water has a lower salinity than the surface water. It is hypothesized that thermocline salinity inversions should generally occur offshore from upwelling regions whenever winds are steady enough and surface warming is sufficiently strong.

1. Introduction

Large upwelling systems such as the Benguela upwelling and the Peruvian upwelling have caught considerable attention during the last decade due to the occurrence of increasing volumes of suboxic water masses [*Mohrholz et al.*, 2008; *Karstensen et al.*, 2008; *Schmidt and Eggert*, 2016; *Thomsen et al.*, 2016]. Generally, high oxygen demand and low ventilation are responsible for this phenomenon [*Brandt et al.*, 2015]. In many of these observational studies one striking feature is present which has however not been further discussed: in the thermocline, a significant salinity maximum is visible; see, e.g., Figure 6b of *Brandt et al.* [2015] for the eastern tropical North Atlantic and Figures 2i and 2j of *Thomsen et al.* [2016] for the Peruvian upwelling system. Older observations show this feature for the Benguela upwelling: Figures 5 and 6 of *Armstrong et al.* [1987].

Also, studies of the smaller upwelling systems in the Baltic Sea show salinity inversions. The Baltic Sea is a semienclosed brackish marginal sea of the North Sea with almost no tides and strong salinity stratification [*Reissmann et al.*, 2009]. Observations by *Lass et al.* [2010] show distinct salinity minima inside the thermocline below the surface mixed layer under upwelling favorable winds, see their Figures 5 and 15. Recently published data from the Gulf of Finland of the Baltic Sea include thermocline salinity minima as well for various summer days in 2010 and 2012; see Figure 7 by *Lips et al.* [2016]. Those observed salinity minima are, however, not further discussed by *Lass et al.* [2010] and *Lips et al.* [2016].

It is the aim of this paper to explain these thermocline salinity minima (midlatitude Baltic Sea) and maxima (tropical and subtropical upwelling systems) by first presenting new data from the central Baltic Sea obtained during a dedicated upper ocean high-resolution campaign (see section 2). With this, we use the semienclosed, nontidal, and easily accessible Baltic Sea as a natural laboratory for understanding processes which are also relevant for the large upwelling systems. Afterward, a simple box model is first constructed (section 3) and then applied (section 4) to explain the generation of salinity minima under these conditions. The results are then discussed in section 5.

2. Observations in the Central Baltic Sea

2.1. Field Program

During 7–15 July 2012, a field campaign with two ships was carried out in the central Baltic Sea. During that period, R/V *Meteor* was located at the fixed position 57.32°N, 20.05°E (identical to the Baltic monitoring station BY15), while sampling high-frequency time series profiles. At the same time, R/V *Elisabeth Mann Borgese* carried out consecutive meridional transects of 10 nautical miles length with high-resolution vertical and horizontal sampling. Here data from a transect along 20.05°E during 2 h on 11–12 July are presented.

Conductivity-temperature-depth (CTD) chain transect. The CTD chain towed by R/V *Elisabeth Mann Borgese* was equipped with 91 sensor fins each placed 1.3 m apart and inductively coupled to the simply coated steel wire. The fins with integrated sensors (i.e., temperature, conductivity, pressure, and oxygen) delivered data of the upper water column every 3 s. Based on the towing speed of 4 knots, this corresponds to a horizontal resolution of 6 m. Along the transect the sensors covered a depth range of approximately 6 m to 95 m yielding a mean vertical resolution of 1 m. The accuracies of the CTD chain measurements are estimated as $\pm$0.02 K and $\pm$0.04 g/kg for temperature and salinity, respectively.

Time series hydrographic data. Time series data at central station in the eastern Gotland basin were gathered with a microstructure profiling probe (MSS) from stern of the R/V *Meteor*. The MSS is a free falling profiler equipped with pressure, temperature, conductivity, and shear sensors. Every second hour a set of three subsequent profiles was obtained within 40 to 60 min. The three profiles were temporally averaged. Thus, the processed time series data have a temporal and vertical resolution of 2 h and 0.5 m, respectively. All sensors were calibrated prior the cruise. The residual absolute uncertainty of temperature and salinity is about 0.01 K and 0.02 g/kg.

Currents. To obtain undisturbed current data from the uppermost layers, a floating drifter with an upward looking Acoustic Doppler Current Profiler (ADCP) at 35 m depth was used. The drifter was deployed at the time series station on 8 July. During the time series measurements the drifter moved slowly southeastward and reached a maximum distance of 8 nautical miles on 14 July. The current data of the 600 kHz Workhorse ADCP covered the depth range between 2 m and 33 m depth with a vertical resolution of 0.5 m. The ADCP measured the current velocity relative to the horizontal movement of the drifter. Its actual position was taken by a GPS receiver on top of the buoy and transmitted via IRIDIUM satellite communication. The drifter speed was calculated from the time series of drifter position. Using these data, the relative current data of the ADCP were corrected with the drifter speed to obtain absolute velocities in Earth coordinates. The current data were vertically averaged between 2 m and 10 m depth to derive the estimate of mixed layer horizontal velocities.

Wind data. The R/V *Meteor* is equipped with a ship weather station operated and maintained by the German Weather Service (DWD). As part of the scientific crew a DWD technician processes all weather data according the standard DWD procedures, including an extrapolation of the wind observations taken in 35 m height to the standard 10 m height. The original data, with a temporal resolution of 1 min, were averaged to 30 min mean values.

2.2. Analysis of Field Data

The field campaign in the central Baltic Sea was carried out during a phase of pronounced southwesterly wind with wind speeds up to 15 m s^{-1}; see Figure 1. This caused an Ekman transport in southeasterly direction with residual current speeds up to 0.1 m s^{-1} in the upper mixed layer. Since the upper 2 m of the water column were not covered by measurements, the observed angle between wind and depth-mean current deviates from the theoretical value of 90°. The offshore Ekman transport results in a strong coastal upwelling along the east coast of the island of Gotland as seen from the SST (sea surface temperature) observations shown in Figure 1. Outside the upwelling region a large-scale temperature gradient in southeasterly direction is visible ranging from about 12°C in the upwelling region to 17°C about 100 km offshore.

The hydrographic transect in Figure 2 (left column) shows a surface mixed layer about 15 m thick with a potential temperature of about 16°C and a salinity of about 7.15 g/kg. In the 5–10 m thick thermocline below, temperature decreases linearly to 6°C causing a stable stratification. The salinity in the thermocline shows distinct salinity minima with values of about 7.0 g/kg; further down salinity increases up to 7.5 g/kg in the winter water. The observed salinity minima are patchy in space but are visible throughout the entire transect. The major goal of this study is to explain the origin of these salinity minima.

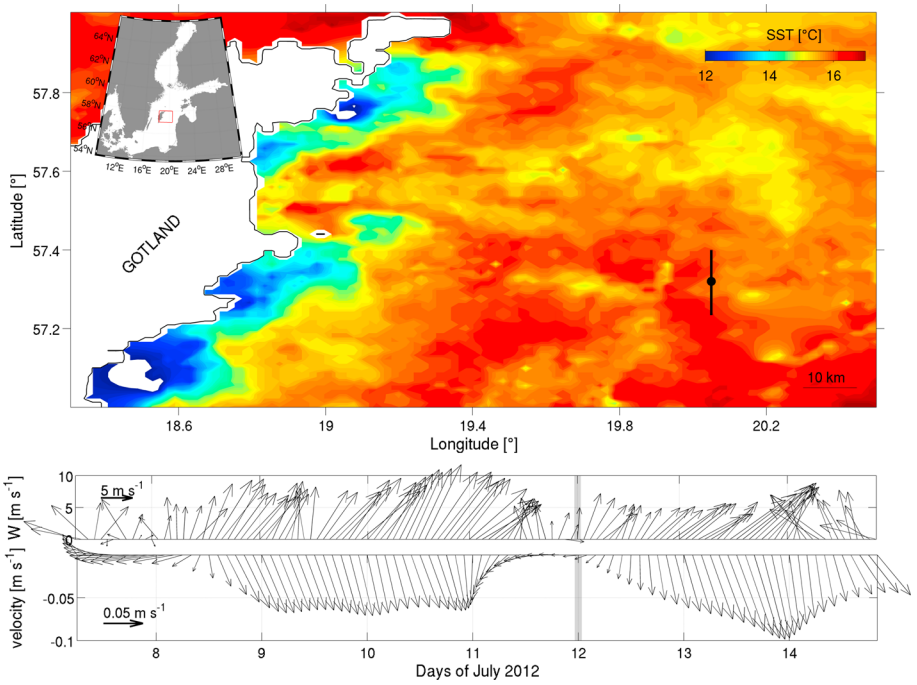

Figure 1. (top) Map of the study area and surface sea temperature retrieved from satellite (Advanced Very High Resolution Radiometer of the U.S. Weather Satellite NOAA 19 and the European weather satellite MetOp-2 are combined to calculate the daily average) on 11–12 July 2012. The black line indicates where the hydrographic transect data were sampled by R/V *Elisabeth Mann Borgese*. The dot on this transect denotes the location where the wind and the hydrographic profile data were collected by R/V *Meteor*. Time series of wind are shown in the middle panel, and mean current in the upper 10 m, filtered to remove the inertial and diurnal cycles, are shown on the bottom panel. The latter were collected from a drift buoy released from the position indicated by the black dot. The gray bar shows the time period during which the transect data shown in Figure 2 have been observed.

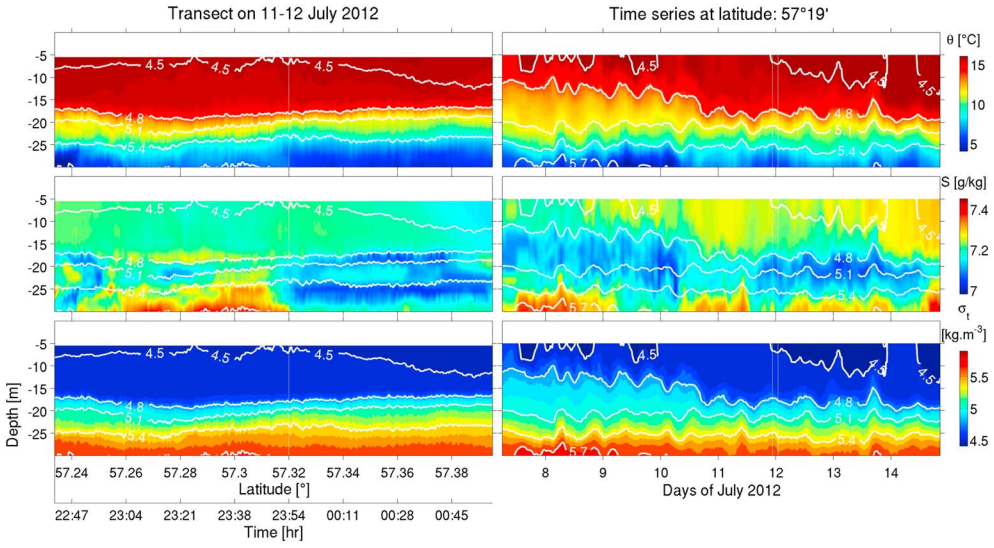

Figure 2. (left column) Spatial and (right) temporal change of (top row) potential temperature, (middle row) absolute salinity, and (bottom row) potential density anomaly. The vertical white line in Figure 2 (left column) shows the time and position, where the transect intersected close to the time series station, and the vertical lines in Figure 2 (right column) indicate the time span when the transect was sampled. The bold white lines in all panels show the isopycnals.

The time series of hydrographic profiles measured in the center of the transect during 8 days (Figure 2, right column) show increasing temperature and salinity in the upper mixed layer, which is deepening from about 10 m to about 20 m during this time. In contrast to the observed trends this entrainment to the thermocline should mix up colder and fresher water masses, which hints to the contribution of other processes within the mixed layer. The thermocline salinity minima are visible throughout the time series with no clear trend, such that the increasing mixed layer salinity causes increase of the salinity difference from about 0.1 g/kg (on 8 July) to about 0.25 g/kg (on 14 July).

It is our hypothesis that the salinity minima in the thermocline are generated by the Ekman transport of upwelled saltier water masses within the surface mixed layer. The net surface warming prevents a destabilization of the stratification in the thermocline. In section 3, we construct a simple box model to quantitatively test this hypothesis.

3. Box Model

A simple box model (see Figure 3 for the geometry) is constructed to explain the observed salinity inversions in the central Baltic Sea during upwelling favorable winds. For each box, budgets of temperature and salinity are calculated in dependence of advective interface fluxes between the boxes or surface fluxes between the atmosphere and the ocean. Advection velocities are calculated from the Ekman transport, and surface fluxes are calculated from bulk formulae. The *upwelling* box A extends perpendicular from the coast at $x = 0$ to the offshore limit of the upwelling region at $x = W_A$ and covers the mixed layer of depth $h_m = 10.0$ m $\pm$ 5.0 m as well as the upper half of the thermocline of thickness $\Delta h = 7.5$ m $\pm$ 2.5 m. The *offshore surface mixed layer* box B extends in seaward direction from the offshore limit of the upwelling region and has a width of $W_B = 150,000$ m $\pm$ 50,000 m and a depth identical to the mixed layer depth h_m. Initial values for the surface salinity and temperature are $(S_u)_0 = 7.0$ g/kg and $(\theta_u)_0 = 16.0$°C, respectively, and temporally constant values in the lower layer are $S_l = 7.5$ g/kg $\pm$ 0.1 g/kg and $\theta_l = 5.0$°C $\pm$ 1.0°C, respectively. A constant wind stress parallel to the coast with the coast to the left, $\tau_s > 0$, is applied which leads to an offshore Ekman transport $U_e = \tau_s/(f\rho_0)$ confined to the surface mixed layer, with the reference density $\rho_0 = 1010$ kg m^{-3} and the Coriolis parameter $f > 0$. The Ekman velocity is $u_e = U_e/(h_m + 0.5\Delta h)$ and the resulting upwelling velocity is $w_e = U_e/W_A$. Including surface heat and freshwater fluxes, and following a finite volume approach, the box-integrated budget equations for potential temperature and salinity are of the following form:

$$\begin{aligned} \frac{\mathrm{d}}{\mathrm{d}t}\left(\theta_u^A\left(h_m+\frac{1}{2}\Delta h\right)W_A\right) &= U_e\left(\theta_{th}^A-\theta_u^A\right)+F_\theta^A W_A;\\ \frac{\mathrm{d}}{\mathrm{d}t}\left(S_u^A\left(h_m+\frac{1}{2}\Delta h\right)W_A\right) &= U_e\left(S_{th}^A-S_u^A\right)+F_S^A W_A, \end{aligned} \tag{1}$$

with the potential temperature and salinity representative for the thermocline underneath box A, $\theta_{\mathrm{th}}^A = \frac{1}{2}(\theta_u^A + \theta_l)$ and $S_{\mathrm{th}}^A = \frac{1}{2}(S_u^A + S_l)$. In (1), $W_A = 5000$ m is the width of the upwelling region, defined here as the internal Rossby radius of the central Baltic Sea, which is about 5 km, according to *Fennel et al.* [1991]. The finite volume budgets for the offshore box B read as

$$\begin{aligned} \frac{\mathrm{d}}{\mathrm{d}t}\left(\theta_u^B h_m W_B\right) &= U_e\left(\theta_u^A-\theta_u^B\right)+F_\theta^B W_B;\\ \frac{\mathrm{d}}{\mathrm{d}t}\left(S_u^B h_m W_B\right) &= U_e\left(S_u^A-S_u^B\right)+F_S^B W_B. \end{aligned} \tag{2}$$

The surface heat flux is expressed as a downward surface temperature flux (warming the surface waters), and the freshwater flux due to net evaporation is expressed as a downward surface salinity flux (making the surface waters saltier). The surface fluxes are calculated by means of the simple bulk formulae provided by *Garratt and Hyson* [1975]. The following atmospheric parameters were used: air pressure $p_{\mathrm{air}} = 1010$ kg m^{-3}, air temperature $T_{\mathrm{air}} = 18.0$°C $\pm$ 2.0°C, specific humidity $q_s = 0.007$, daily mean incoming shortwave radiation $\bar{Q}_s = 223.0$ W m^{-2}, total cloud cover tcc = 0.5, precipitation $P = 1.9 \cdot 10^{-8}$ m s^{-1}, and wind speed $W = 8.0$ m s^{-1} $\pm$ 2.0 m s^{-1}. For the calculation of density, a linear equation of state is used:

$$\rho(\theta, S) = \rho_0\left(1 + \alpha(\theta - \theta_l) + \beta(S - S_l)\right) \tag{3}$$

with the thermal expansion coefficient, $\alpha = -2 \cdot 10^{-4}$ K^{-1}, and the haline contraction coefficient, $\beta = 7 \cdot 10^{-4}$ (g/kg)$^{-1}$.

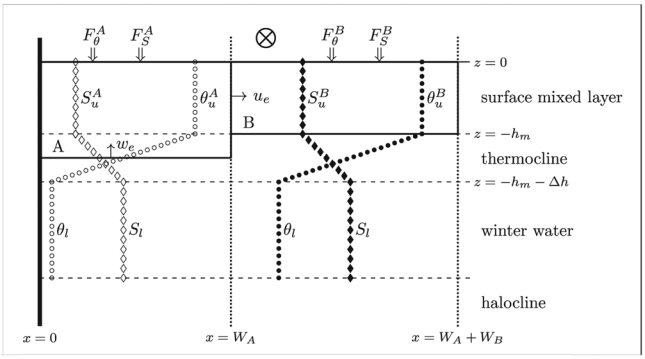

Figure 3. Sketch of the box model showing initial profiles of potential temperature and salinity for (left) the upwelling box A and (right) the offshore box B.

The question is under which circumstances the mixed layer salinity of box B can be larger than the thermocline salinity underneath the surface mixed layer of box B, S^B_{th} without destabilizing the thermocline stratification? That is,

$$S^B_{th} < S^B_u \text{ and } \rho^B_{th} > \rho^B_u, \tag{4}$$

where the thermocline values in box B, $\theta^B_{th} = 12.0°\text{C}$, and $S^B_{th} = 7.15$ g/kg are taken from observations; see Figure 2. These values are used for diagnostics only.

4. Model Simulations

To include an uncertainty analysis into the model simulation, 1000 model experiments are executed where the following model parameters are varied independently: h_m, Δh, W_B, S_l, θ_l, T_{air}, and W. Random numbers were drawn from a uniform distribution with mean value and range given in section 3. This Monte Carlo type of analysis allows evaluating mean time series for mean potential temperature, salinity, and potential density and their standard deviation.

Initial surface potential temperature and salinity are not varied, since this is already done for the lower layer temperature and salinity as well as for the air temperature. The mean values and their variations have been estimated from the observations shown in Figure 2 as well as from model simulations by *Holtermann et al.* [2014] and *Gräwe et al.* [2015], which cover the central Baltic Sea during July 2012. Mean air temperature is chosen such that net surface heat flux is zero in the absence of Ekman forcing.

Initially, profiles of salinity and potential temperature are stably stratified with $(S_u)_0 < S_l$ and $(\theta_u)_0 > \theta_l$, which corresponds to typical summer conditions with winter water overlaid by thermocline; see section 1.

Figure 4 shows the results for mean values and their standard deviation during 14 days of simulations using the box model with and without surface heat and freshwater fluxes. After initialization, salinity and density increase and temperature decreases quickly during the first 3 days in the upwelling box A (red lines) and afterward slowly converge toward the lower layer values, such that box A becomes almost homogenized. With some delay, surface salinity, temperature, and density in the surface mixed layer of box B react to the changed water properties in the upwelling box A. Without surface fluxes, salinity stratification is inverted in box B after 9 days (−3 days/+5 days; $S^B_u > S^B_{th}$; see Figure 4a), but density and a little later also temperature are inverted ($\theta^B_u > \theta^B_{\text{th}}$ and $\rho^B_u > \rho^B_{\text{th}}$; see Figures 4b and 4c), such that an unrealistic unstable stratification would occur.

When applying surface fluxes, the resulting maximum downward net surface heat flux results in 350 W m^{-2} for the upwelling box A and 110 W m^{-2} for the offshore box B, starting from zero fluxes at the initialization of the model. Surface freshwater fluxes varied around zero do not significantly change salinity, whereas downward heat fluxes increase potential temperature in the offshore box B by about 2.5 K from 11°C ± 2.0°C to 13.5°C ± 1.0°C, and density is consequently decreased in average by about 0.4 kg m^{-3} after 14 days. This leads to a salinity inversion (again after 9 days; −3 days/+5 days), while temperature and density remain stably stratified in average.

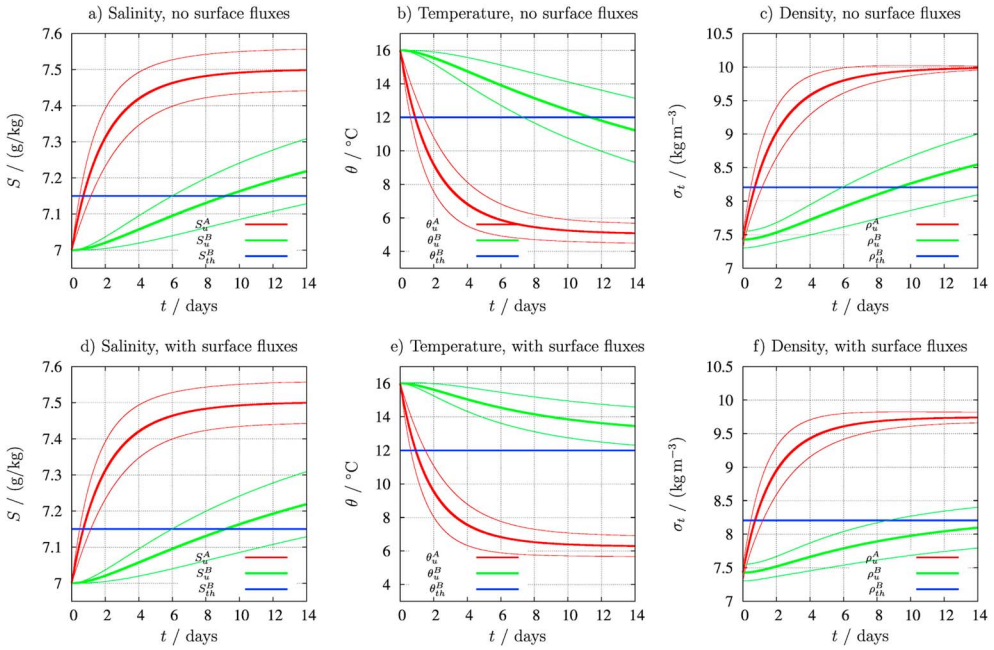

Figure 4. Time series of (a, d) salinity, (b, e) potential temperature, and (c, f) potential density during 14 days as calculated by means of the box model. Bold lines represent mean values, and thin lines indicate the range of one standard deviation. Red lines represent surface values in the upwelling box A, and green lines represent values in the surface mixed layer box B. The blue lines indicate the constant thermocline values underneath box B. Figures 4a–4c show results for zero surface fluxes of freshwater and heat, and Figures 4d–4f show results for nonzero surface fluxes.

Entrainment, which is neglected in these simple box model simulations, would have the effect of increased flux of thermocline waters into the upper mixed layer of box B as well as the deepening of the surface mixed layer. Such effects are already included by the Monte Carlo simulations by varying wind speed and mixed layer depth. One characteristic of the observations which could not be reproduced by the model is the increase of the SST, an effect which probably is triggered by either other more complex advective patterns or nonconstant meteorological conditions.

5. Discussion

In strongly stratified thermoclines, salinity almost behaves like a passive tracer with only small impact on potential density. As such, it does not matter much dynamically, whether or not salinity of upwelled water is higher or lower than the surface waters. When it is higher than in the surface waters such as in the Baltic Sea, salinity minima occur when saltier water, warmed due to surface heat fluxes, is transported over the older surface waters [*Lass et al.*, 2010; *Lips et al.*, 2016, this study]. In contrast, as, for example, in the eastern tropical North Atlantic [*Brandt et al.*, 2015], the Benguela upwelling system [*Armstrong et al.*, 1987], and the Peruvian upwelling system [*Thomsen et al.*, 2016], upwelled water is less salty than surface waters such that the same process of offshore Ekman transport and surface warming leads to salinity maxima in the thermocline. We therefore hypothesize that such salinity inversions should be a general feature of the region offshore from the upwelling region, when upwelling favorable winds are sufficiently steady and surface warming is strong enough.

Since salinity is inert, the presence and maintenance of salinity inversions is indicative for the relatively low intensity of vertical and lateral mixing processes in the thermocline. Figure 2 shows that thermocline salinity has high spatial and temporal variability. Determination of the decay rate of this variability could help to estimate efficiency of diapycnal mixing (e.g., due to breaking of internal waves) and isopycnal mixing (e.g., due to submesoscale eddies). Also, the dynamics of lateral intrusions within the thermocline could be studied. The effect of strong lateral mixing is included in the simple box model of section 3 due to the width of the offshore box and the upstream type of advection scheme used. A simple Lagrangian thought experiment can help to understand what would happen without any lateral mixing: assume that upwelled water is simply moving

offshore and warming up due to a constant surface heat flux $\bar{Q}$. Then this new surface water would have the following potential temperature θ_u and salinity S_u:

$$\theta_u \longrightarrow \theta_l + \Delta t \frac{\bar{Q}}{C_p \rho_0 h_m}; \quad S_u \longrightarrow S_l, \tag{5}$$

where Δt is the time elapsed since first surface contact. With the condition for reaching stable salinity minima in the thermocline, $\rho_u < \rho_{\text{th}}$ and $S_u > S_{\text{th}}$, and inserting this condition into the equation of state (3), using (5), the following time duration is needed to reach this stable state:

$$\Delta t = \left\{ \frac{\beta}{-\alpha} \left(S_l - S_{\text{th}}\right) - \left(\theta_l - \theta_{\text{th}}\right) \right\} \frac{C_p \rho_0 h_m}{\bar{Q}}. \tag{6}$$

When assuming an average of $\bar{Q} = 100$ W/m^2, and inserting values from section 3 into 6, a necessary time span of $\Delta t = 28$ days would be needed. This is substantially more than the time of about 7 days resulting from the box model with a comparable mean value of surface heat flux, as seen from Figure 4. This discrepancy can only be explained by lateral mixing missing in this Lagrangian thought experiment. Such a lateral mixing is implicitly included in the box model due to numerical mixing which can be quantified for the underlying first-order upstream scheme at relatively small time step as a numerical diffusivity of $K_h = 0.25 u_e (W_A + W_B)$ [see, e.g., *Smolarkiewicz*, 1983]. Using the values applied here, the box model results in a numerical diffusivity of $K_h = 2372$ m^2 s$^{-1} \pm 1104$ m^2 s^{-1}. *Zhurbas et al.* [2008] estimate for the Gulf of Finland an effective diffusivity of 500 m^{2}s^{-1}, such that for the larger Central Baltic Sea an order of 10^3 m^2 s^{-1} could give a realistic value. The quantification of lateral mixing, which is assumed to play a major role for establishing salinity inversions in the thermocline, requires further studies in upwelling regions. With this, it will be a future challenge to numerically simulate the generation and dynamics of the observed salinity inversions by means of a realistically forced regional ocean model.

Acknowledgments
This paper is a contribution to the project T2 (energy budget of the ocean surface mixed layer) of the Collaborative Research Centre TRR 181 on Energy Transfer in Atmosphere and Ocean funded by the German Research Foundation. We are grateful to Herbert Siegel (Warnemünde) for providing the satellite data for Figure 1 and to Peter Holtermann (Warnemünde) for giving insight into his model results. The observational data on which this study is based are available by request to the corresponding author (hans.burchard@io-warnemuende.de).

References

Armstrong, D., B. Mitchell-Innes, F. Verheye-Dua, H. Waldron, and L. Hutchings (1987), Physical and biological features across an upwelling front in the southern Benguela, *S. Afr. J. Mar. Sci.*, *5*, 171–190.

Brandt, P., et al. (2015), On the role of circulation and mixing in the ventilation of oxygen minimum zones with a focus on the eastern tropical North Atlantic, *Biogeosciences*, *12*, 489–512.

Fennel, W., T. Seifert, and B. Kayser (1991), Rossby radii and phase speeds in the Baltic Sea, *Cont. Shelf Res.*, *11*, 23–36.

Garratt, J., and P. Hyson (1975), Vertical fluxes of momentum, sensible heat and water vapour during the Air Mass Transformation Experiment (AMTEX) 1974, *J. Meteorol. Soc. Jpn.*, *53*(2), 149–160.

Gräwe, U., P. L. Holtermann, K. Klingbeil, and H. Burchard (2015), Advantages of vertically adaptive coordinates in numerical models of stratified shelf seas, *Ocean Modell.*, *92*, 56–68.

Holtermann, P. L., H. Burchard, U. Gräwe, K. Klingbeil, and L. Umlauf (2014), Deep-water dynamics and boundary mixing in a nontidal stratified basin: A modeling study of the Baltic Sea, *J. Geophys. Res.*, *119*, 1465–1487, doi:10.1002/2013JC009483.

Karstensen, J., L. Stramma, and M. Visbeck (2008), Oxygen minimum zones in the eastern tropical Atlantic and Pacific Oceans, *Progr. Oceanogr.*, *77*, 331–350.

Lass, H.-U., V. Mohrholz, G. Nausch, and H. Siegel (2010), On phosphate pumping into the surface layer of the eastern Gotland Basin by upwelling, *J. Mar. Syst.*, *80*, 71–89.

Lips, U., V. Kikas, T. Liblik, and I. Lips (2016), Multi-sensor in situ observations to resolve the sub-mesoscale features in the stratified Gulf of Finland, Baltic Sea, *Ocean Sci.*, *12*, 715–732.

Mohrholz, V., C. Bartholomae, A. Van der Plas, and H. Lass (2008), The seasonal variability of the northern Benguela undercurrent and its relation to the oxygen budget on the shelf, *Cont. Shelf Res.*, *28*, 424–441.

Reissmann, J. H., H. Burchard, R. Feistel, E. Hagen, H. U. Lass, V. Mohrholz, G. Nausch, L. Umlauf, and G. Wieczorek (2009), Vertical mixing in the Baltic Sea and consequences for eutrophication—A review, *Progr. Oceanogr.*, *82*, 47–80.

Schmidt, M., and A. Eggert (2016), Oxygen cycling in the northern Benguela upwelling system: Modelling oxygen sources and sinks, *Progr. Oceanogr.*, *149*, 145–173.

Smolarkiewicz, P. (1983), A positive definite advection scheme with small implicit diffusion, *Mon. Weather Rev.*, *111*, 479–486.

Thomsen, S., T. Kanzow, F. Colas, V. Echevin, G. Krahmann, and A. Engel (2016), Do submesoscale frontal processes ventilate the oxygen minimum zone off Peru?, *Geophys. Res. Lett.*, *43*, 8133–8142, doi:10.1002/2016GL070548.

Zhurbas, V. M., J. Laanemets, N. P. Kuzmina, S. S. Muraviev, and J. Elken (2008), Direct estimates of the lateral eddy diffusivity in the Gulf of Finland of the Baltic Sea (based on the results of numerical experiments with an eddy resolving model), *Oceanologia*, *48*, 175–181.